Design of Radial Microstrip Band Pass Filter with Wide Stop-Band Characteristics for GPS Application

Prashant K. Singh[*]**, Anjini K. Tiwary, and Nisha Gupta**

Abstract—In this paper, a novel compact band pass filter (BPF) is proposed for Global Positioning System (GPS) receivers. The proposed BPF configuration is composed of a low pass filter (LPF) section formed by the coupled line transformer connected with a radial stub and two short circuited stubs embedded within the $50\,\Omega$ microstrip line connecting the input/output (I/O) port of LPF. The lumped equivalent model of proposed BPF is also presented and analyzed. Simulation as well as experimental results shows very good in-band (pass-band) and out-of-band ($\approx 7f_c$ (centre frequency)) characteristics. The 3 dB fractional bandwidth (FBW) is 3.2% of f_c, thus satisfying the GPS receiver requirement and the minimum insertion loss (IL) in pass-band is 1.28 dB.

1. INTRODUCTION

Modern microwave/wireless communication transceivers require low cost and compact band pass filters (BPF) with good pass-band and ultra-wide out-of-band (stop-band) characteristics that can be fabricated easily. Achieving all these requirements simultaneously is a real challenging task to the researchers. However, planar BPFs are in demand due to their easy fabrication. Various applications like wireless personal communication services (PCS), global system for mobile communications (GSM) and GPS needs narrowband BPFs. The GPS has now become the integral part of our day to day life due to its various navigational applications. The frequency band allotted for GPS receiver system is 1.559 GHz–1.610 GHz [1]. According to the need of narrowband BPFs in terms of better performance or size miniaturization various designs have been proposed [2–18]. The stepped impedance parallel coupled resonators are used for suppression of harmonics in BPF [2]. Cross coupled branch line resonators are used to design narrowband BPF with ultra-wide stop-band by generating number of transmission zeroes in stop-band [3]. However, stepped impedance resonators and branch line resonators increase the circuit size. For size miniaturization, meander line [4] and meander loop resonators [5, 6] are proposed for designing narrowband BPFs, but at the cost of poor out-of-band performance. For high selectivity various cascaded quadruplet BPFs [7–9] based on quarter wave resonators are proposed, while the circuits incorporated are complex and large. Open/shorted dual behavior resonators [10] are used to enhance the stop-band of BPF, which causes the increase in size of the filter. Compact narrowband BPFs are also designed using two stub loaded open loop resonator [11] and hybrid resonator [12] with good in-band characteristic at the cost of out-of-band characteristic lower than $4f_c$. Other methods for size miniaturization and harmonic suppression use defected ground structure (DGS) [13] and radial stub [14–16]. By combining both techniques DGS and radial stub, miniaturized dual-mode ring BPFs with wide stop-band have also been proposed [17, 18]. However, DGS has disadvantages of extra radiation due to partially open ground plane and complex fabrication as the alignment of top microstrip structure and ground slots must be precise enough to minimize the fabrication error. Planar radial stubs on the other

hand [19–23], are very good choice for designing the compact BPFs with good in-band and out-of-band characteristics.

In this work, a novel compact and narrowband BPF with ultra-wide stop-band is proposed for GPS receiver (1.559 GHz–1.610 GHz) application. The proposed structure uses planar microstrip configuration composed of coupled line transformer connected with radial stub and two short circuited stubs embedded within the $50\,\Omega$ microstrip line connecting the two I/O ports. The transformer connected with radial stub provides ultra-wide stop-band as well as compact structure, while embedded short circuited stubs realizes the BPF response. The proposed configuration printed over the dielectric substrate has several advantages such as easier fabrication, compact structure, low cost, ultra-wide stop-band (up to $7f_c$), low insertion loss (1.28 dB) at f_c in pass-band, good reflection loss (18 dB) in pass-band and good insertion loss in stop-band (> 15 dB).

2. DESIGN AND SIMULATION RESULT

The proposed compact and narrowband band pass filter (BPF) for GPS receiver with ultra-wide stop-band is designed using the short circuited stubs (inductive via line) loaded at I/O port of the low pass filter (LPF) configuration formed by the coupled line transformer connected with a radial stub. The two short circuited stubs are embedded within the $50\,\Omega$ microstrip line connecting the two ports of the filter. In this section, first lumped model is analyzed and then using the lumped model analysis microstrip model is investigated. The lumped models are designed, simulated and analyzed using ADS2009 (Advanced Design System 2009) software by Agilent Technologies. The microstrip structures are designed and simulated on IE3D, full wave method of moments (MoM) based simulation software by Zeland. The substrate used for all microstrip structures is RT/duroid RO5880 substrate of dielectric constant $= 2.2$, thickness $= 1.57$ mm and loss tangent $= 0.0009$.

The LPF section used for designing the proposed BPF is shown in Figure 1 and its lumped equivalent is shown in Figure 2. The LPF section with ultra-wide stop-band can be designed by using the transmission line elements (coupled line, transmission line and radial stub), which can be represented by lumped elements in certain frequency range [14–16]. The radial stub used in filter configuration can be analyzed as a series combination of an inductor and a capacitor and their value of input impedance (Z_{in}), inductance (L_r) and capacitance (C_r) can be calculated as [24]:

$$Z_{in} \cong -j\frac{120\pi h\beta}{\theta_r\sqrt{\varepsilon_{eff}}}\left(\ln\frac{r_i}{r_o} + \frac{1}{2} + \frac{2}{\beta r_o^2}\right) \tag{1}$$

$$L_r = \frac{120\pi h}{\theta_r c}\left[\ln\frac{r_o}{r_i} - \frac{1}{2}\right] \tag{2}$$

$$C_r = \frac{\theta_r r_o^2 \varepsilon_{eff}}{240\pi hc} \tag{3}$$

where, h is the dielectric thickness, β the phase constant, θ_r the spanning angle in radian, c the speed of light, ε_{eff} the effective dielectric constant, r_i the inner radius of radial stub and r_o the outer radius of radial stub.

Using the design equations [14–16, 24], the design parameters of microstrip LPF for 3-dB cut-off frequency of 1.8 GHz are obtained as $r_o = 8.5$ mm, $r_i = 0.6$ mm, $\theta_r = 135°$, $w_1 = 4.84$ mm, $w_2 = 0.4$ mm, $s = 0.3$ mm, $l_v = 7$ mm, $l_h = 0.8$ mm, $l_2 = 2.42$ mm and $l_3 = 7$ mm. The lumped parametric values for the LPF are $L_r = 2.16$ nH, $C_r = 1.2$ pF, $L = 5.22$ nH, $C_{p1} = 0.081$ pF, $C_m = 0.05$ pF, $k = 0.38$, $C_{p2} = 0.001$ pF, $L_s = 0.48$ nH and $C_p = 0.082$ pF.

Next, a slot is etched out in the $50\,\Omega$ microstrip line of this LPF; the structure still works as LPF. Further, a high impedance short circuited transmission line is embedded within this slot as shown in Figure 3. This shunt inductive lines located at the two input-output ports, ground some range of lower frequency signal starting from DC signal in lower portion of the pass-band of LPF without disturbing the stop-band characteristics of the LPF. Hence the proposed structure passes a specific band of signal and it works as band pass filter (BPF) with ultra-wide stop-band.
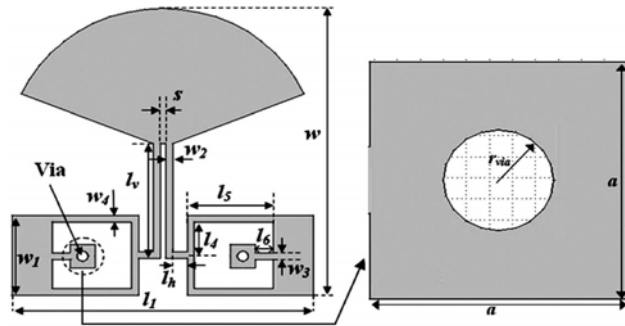
The lumped equivalent model of proposed microstrip configuration is shown in Figure 4. The section with dimensions l_6 and $(l_4 + l_5)$ denotes equivalent series inductances L_a and L_b connected to
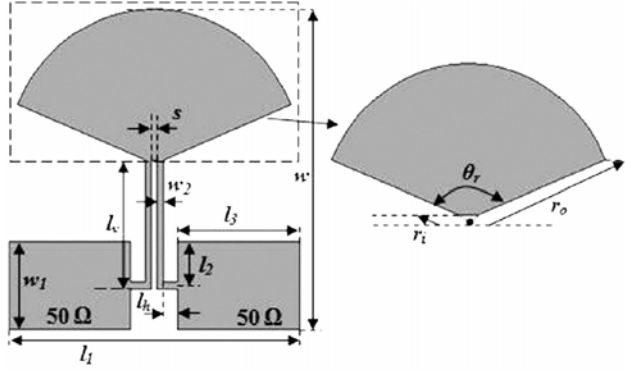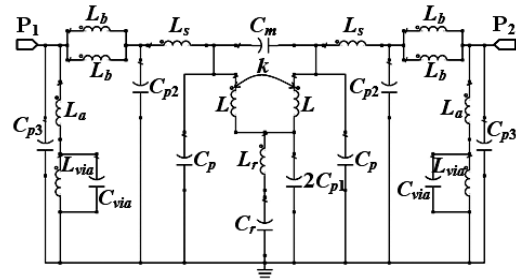
Figure 1. Microstrip LPF with $l_1 = 16.7\,\text{mm}$ and $w = 17.5\,\text{mm}$.
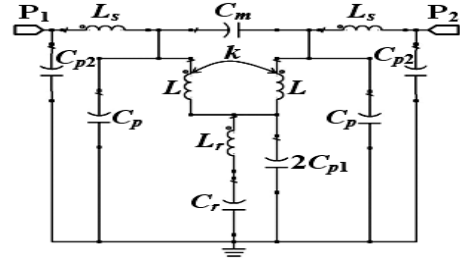
Figure 2. Lumped model of microstrip LPF.

Figure 3. Proposed microstrip BPF with $l_1 = 16.7\,\text{mm}$ and $w = 17.5\,\text{mm}$.

Figure 4. Lumped equivalent model of proposed BPF.

shunt parasitic capacitances respectively. While inset section is equivalent to the parallel combination of inductance (L_{via}) and capacitance (C_{via}) and are given by [23, 25]:

$$L_{via} = \frac{\mu_o}{2\pi}\left[h\ln\left(\frac{h + \sqrt{r_{via}^2 + h^2}}{r_{via}}\right) + \frac{3}{2}\left(r_{via} - \sqrt{r_{via}^2 + h^2}\right)\right](H) \tag{4}$$

$$C_{via} = \varepsilon_o \varepsilon_r \frac{\left[a^2 - 4\pi r_{via}^2\right]}{h}(F) \tag{5}$$

The bandwidth (BW) of the pass-band and centre frequency (f_c) can be controlled by varying the inductances L and L_a depicted in lumped equivalent model. Initially, L_a is varied by keeping the values of the other design parameters constant as; $L_r = 2.16\,\text{nH}$, $C_r = 1.2\,\text{pF}$, $L = 5.22\,\text{nH}$, $C_{p1} = 0.081\,\text{pF}$, $C_m = 0.05\,\text{pF}$, $k = 0.38$, $C_{p2} = 0.025\,\text{pF}$, $C_p = 0.082\,\text{pF}$, $C_{p3} = 0.06\,\text{pF}$, $L_s = 0.48\,\text{nH}$, $L_b = 4.74\,\text{nH}$, $L_{via} = 0.35\,\text{nH}$ and $C_{via} = 0.01\,\text{nH}$. The transmission characteristic of BPF with variation in L_a is shown in Figure 5. It is seen that, as the inductance value of L_a decreases, the lower 3 dB cut-off frequency shift toward higher frequency side without affecting the upper 3 dB cut-off frequency. The overall effect is the narrow pass-band BW and shifting of centre frequency towards higher frequency region with decrease in L_a.

Further, the inductance value of L is varied by keeping the values of other design parameters constant as; $L_r = 2.16\,\text{nH}$, $C_r = 1.2\,\text{pF}$, $L_a = 6\,\text{nH}$, $C_{p1} = 0.081\,\text{pF}$, $C_m = 0.05\,\text{pF}$, $k = 0.38$, $C_{p2} = 0.025\,\text{pF}$, $C_p = 0.082\,\text{pF}$, $C_{p3} = 0.06\,\text{pF}$, $L_s = 0.48\,\text{nH}$, $L_b = 4.74\,\text{nH}$, $L_{via} = 0.35\,\text{nH}$ and $C_{via} = 0.01\,\text{nH}$. Transmission characteristic for the variation of L is shown in Figure 6, which shows that, with the increase in the value of L, upper 3 dB cut-off frequency shifts towards the lower frequency portion without affecting the lower 3 dB cut-off frequency. Hence the narrow pass-band BW and the shift in centre frequency towards lower frequency portion are seen with the increase in L.
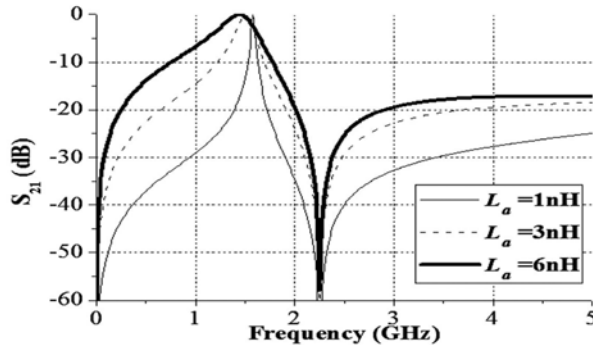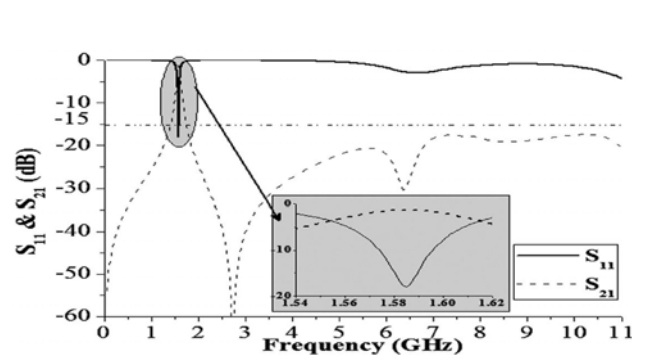
Figure 5. Transmission characteristic of BPF with varying L_a.
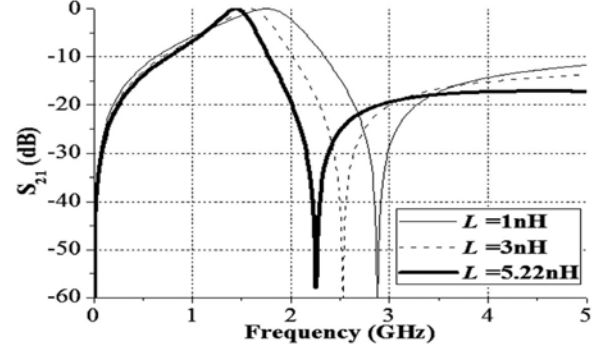
Figure 6. Transmission characteristic of BPF with the variation in L.
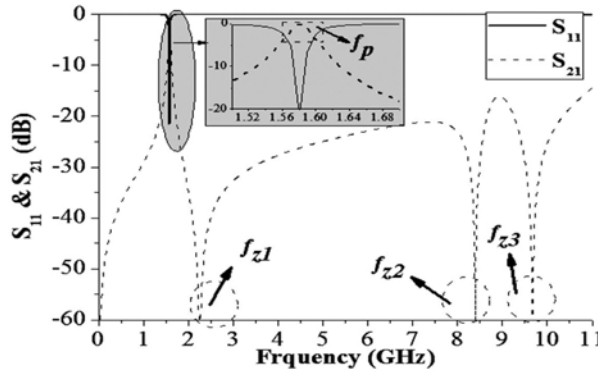
**Figure 7.** Simulation result of lumped model of proposed BPF.

Figure 8. Simulation result of proposed microstrip BPF.

From the above discussion, it is clear that the BW and centre frequency can be controlled by varying two elemental values namely L and L_a. In microstrip configuration these two inductances L and L_a depends on the microstrip section with dimensions $l_v \times w_2$ and $l_6 \times w_3$ respectively. Using the analysis stated as above, the lumped parameter for the proposed BPF for GPS receiver application are obtained as $L_r = 2.16\,\text{nH}$, $C_r = 1.2\,\text{pF}$, $L = 5.22\,\text{nH}$, $C_{p1} = 0.081\,\text{pF}$, $C_m = 0.05\,\text{pF}$, $k = 0.38$, $C_{p2} = 0.025\,\text{pF}$, $C_p = 0.082\,\text{pF}$, $C_{p3} = 0.06\,\text{pF}$, $L_s = 0.48\,\text{nH}$, $L_a = 1\,\text{nH}$, $L_b = 4.74\,\text{nH}$, $L_{via} = 0.35\,\text{nH}$ and $C_{via} = 0.01\,\text{nH}$. The simulation result for the lumped model of proposed BPF for GPS receiver application is shown in Figure 7. The calculated values of the geometrical parameters of proposed BPF as shown in Figure 3 are $r_o = 8.5\,\text{mm}$, $r_i = 0.6\,\text{mm}$, $\theta_r = 135°$, $w_1 = 4.84\,\text{mm}$, $w_2 = w_3 = w_4 = 0.4\,\text{mm}$, $s = 0.3\,\text{mm}$, $a = 1.4\,\text{mm}$, $r_{via} = 0.3\,\text{mm}$, $l_v = 7\,\text{mm}$, $l_h = 0.8\,\text{mm}$, $l_4 = 2.2\,\text{mm}$, $l_5 = 4.78\,\text{mm}$ and $l_6 = 0.98\,\text{mm}$. Simulation result for proposed microstrip BPF is shown in Figure 8.

The simulation result of proposed microstrip BPF shows the 3 dB pass-band BW from 1.559 GHz to 1.610 GHz; the frequency band used in GPS receiver. However, other applications may demand for the enhancement of the selectivity of the filter, which may be met by introducing more number of poles in the pass-band. An ultra-wide stop-band upto 11 GHz with insertion loss (S_{21}) below 15 dB in stop-band is also observed. The insertion loss (S_{21}) of 1.2 dB at centre frequency 1.58 GHz in pass-band and the reflection loss (S_{11}) at 1.58 GHz is 18 dB are also good.

3. EQUIVALENT MODEL ANALYSIS

As the proposed microstrip BPF is symmetrical, even-mode and odd-mode analysis can be used to analyze the filter configuration. The even-mode and odd-mode circuits can be extracted from the equivalent circuit of proposed BPF shown in Figure 4. The even-mode and odd-mode circuits of the
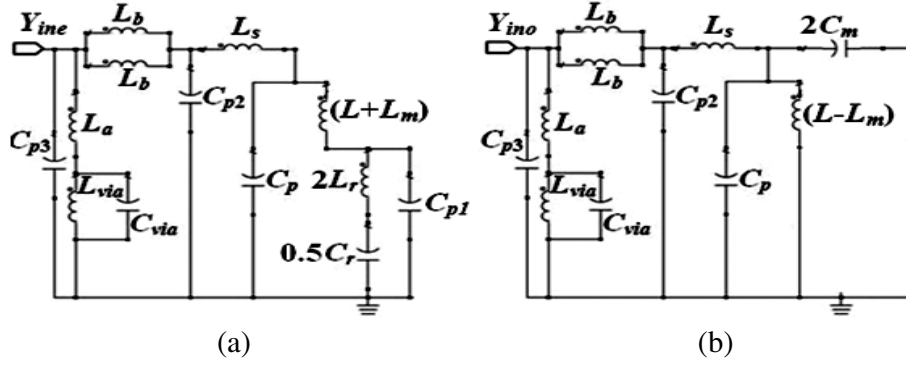
Figure 9. Equivalent circuits of proposed BPF. (a) Even-mode circuit. (b) Odd-mode circuit.

proposed BPF are shown in Figure 9.

The even-mode and odd-mode admittances of the circuit can be calculated as:

$$Y_{ine} = sC_{p3} + \cfrac{1}{sL_a + \cfrac{1}{sC_{via} + \cfrac{1}{sL_{via}}}} + \cfrac{1}{\cfrac{sL_b}{2} + \cfrac{1}{sC_{p2} + \cfrac{1}{sL_s + \cfrac{1}{sC_p + \cfrac{1}{s(L+L_m) + \cfrac{1}{sC_{p1} + \cfrac{1}{2\left(sL_r + \cfrac{1}{sC_r}\right)}}}}}}} \tag{6}$$

$$Y_{ino} = sC_{p3} + \cfrac{1}{sL_a + \cfrac{1}{sC_{via} + \cfrac{1}{sL_{via}}}} + \cfrac{1}{\cfrac{sL_b}{2} + \cfrac{1}{sC_{p2} + \cfrac{1}{sL_s + \cfrac{1}{s(C_p + 2C_m) + \cfrac{1}{s(L - L_m)}}}}} \tag{7}$$

By calculating the even-mode and odd-mode admittances from Equations (6)–(7), the S-parameter can be obtained [26] as:

$$S_{21} = \frac{Y_o Y_{ino} - Y_o Y_{ine}}{(Y_o + Y_{ine})(Y_o + Y_{ino})} \tag{8}$$

$$S_{11} = \frac{Y_o^2 - Y_{ine}Y_{ino}}{(Y_o + Y_{ine})(Y_o + Y_{ino})} \tag{9}$$

The transmission zeroes are generated in stop-band, when $S_{21} = 0$, i.e., even-mode and odd-mode admittances are equal.

$$Y_{ine} = Y_{ino} \tag{10}$$

The transmission poles are generated in pass-band, when $S_{11} = 0$, which gives:

$$Y_o^2 = Y_{ine}Y_{ino} \tag{11}$$

By using Equations (6)–(7), Equation (10) can be written as:

$$2s^6(L_r C_r C_{p1} C_m(L^2 - L_m^2)) + s^4((2C_{p1}C_m + C_r C_m)(L^2 - L_m^2) + 2L_r C_r(LC_m - L_m C_m + L_m C_{p1}))$$
$$+s^2(2LC_m + L_r C_r + L_m(2C_{p1} - 2C_m + C_r)) + 1 = 0 \tag{12}$$

Here, Equation (12) is a 6-degree equation of $s = j2\pi f$, offering 3 positive roots and 3 negative roots for frequency (f). By substituting the values of all the inductances and capacitances as used in

equivalent model of the proposed BPF for GPS application and discarding the negative roots; the three roots are obtained as 2.2 GHz (f_{z1}), 8.3 GHz (f_{z2}) and 9.6 GHz (f_{z3}). Hence the transmission zeroes are obtained at these frequencies encircled as shown in Figure 7. It is clear from the Equation (12), that all the inductance and capacitances responsible for the generation of transmission zeroes in stop-band are elements of LPF section. Hence the proposed BPF retains the ultra-wide stop-band characteristic of LPF. The detailed analysis of the role of the transmission zeros used in LPF section is already studied [14, 16]. The frequency (f_p), at which transmission pole in pass-band is generated, can be calculated using Equations (6)–(7) and (11). Using these equations and substituting the values of all inductances and capacitances used in equivalent model of the proposed BPF for GPS application, the transmission pole is obtained at 1.58 GHz designated as f_p as shown in Figure 7. These equations along with other parameters show that the pass-band also depends on L_{via}, C_{via}, L_a and L_b. The variation of BW and f_c of the BPF is already dealt with in Section 2.

4. EXPERIMENTAL RESULT

After analyzing and designing the proposed microstrip BPF for GPS receiver application, it is further fabricated and tested. The fabricated prototype model of the proposed microstrip BPF is shown in Figure 10. The measurement of transmission and reflection characteristics of the fabricated filter is performed using the Vector Network Analyzer (VNA). The simulation and experimental results of the proposed filter are compared and validated as is shown in Figure 11. The enlarged view of the pass-band region is also depicted in Figure 11. The experimental result is in good agreement with the simulation result thus validating the design of the proposed BPF.

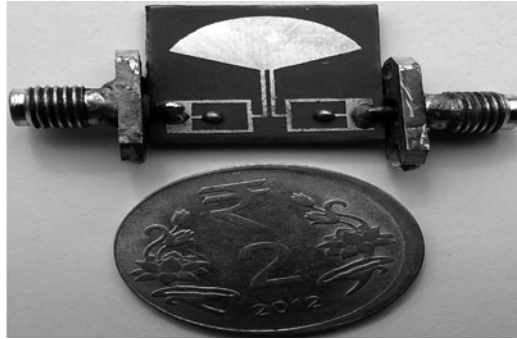The characteristics of the proposed BPF are finally compared with the characteristics of the BPF

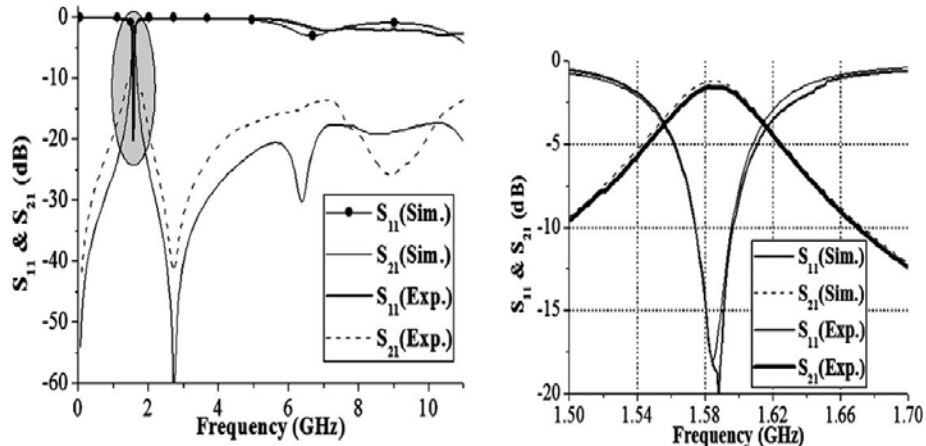**Figure 10.** Fabricated prototype model of the proposed BPF.

Figure 11. Transmission and reflection characteristics of simulation and experiment.

Table 1. Comparison of narrowband BPF.

	f_c (GHz)	Pass-band FBW (%)	Min. IL (dB)	Stop-band suppression level	Size (mm²)
[3]	2	5.9	2.6	27 dB up to $2.88 f_c$	45.4×35.6
[9]	1.503	10.18	1.28	10 dB up to $1.7 f_c$	32.8×25.8
[10]	3	8.3	< 2.2	15 dB up to $2.72 f_c$	35×27
[18]	1.655	2	2.49	10 dB up to $2.24 f_c$	19.9×19.9
Proposed work	**1.58**	**3.2**	**1.28**	**15 dB up to $6.9 f_c$**	**16.7×17.5**

configurations available in the literature. The results are tabulated and compared in Table 1.

The comparison table clearly depicts the superiority of the proposed design in terms of compactness, pass-band as well as stop-band characteristics.

5. CONCLUSION

A compact and narrowband BPF for GPS receiver (1.559 GHz–1.610 GHz) application having ultra-wide stop-band up to 11 GHz is designed, analyzed, fabricated and finally tested. The simulations as well as the equivalent circuit models are presented, and the design is also validated experimentally. The 3 dB fractional bandwidth (FBW) of the proposed BPF is 3.2 % of f_c, and the area occupied by this BPF is only $292.25 \, \text{mm}^2$ $(= l_1 \times w)$.

REFERENCES

1. Chaduc, J.-M. and G. Pogorel, *The Radio Spectrum*, Jhon-Wiley & Sons. Inc., USA, 2008.
2. Worapishet, A., K. Srisathit, and W. Surakampontorn, "Stepped-impedance coupled resonators for implementation of parallel coupled microstrip filters with spurious band suppression," *IEEE Trans. on Microw. Theory and Tech.*, Vol. 60, No. 6, 1540–1548, 2012.
3. Deng, P.-H. and J.-T. Tsai, "Design of microstrip cross-coupled bandpass filter with multiple independent designable transmission zeros using branch-line resonators," *IEEE Microw. and Wire. Comp. Lett.*, Vol. 23, No. 5, 249–251, 2013.
4. Hejazi, Z. M. and A. Omar, "Modeling and simulation of novel ultra-narrowband miniature microstrip filters for mobile and wireless critical applications," *Microw. and Opt. Tech. Lett.*, Vol. 45, No. 1, 35–39, 2005.
5. Esfeh, B. K., A. Ismail, R. S. A. Raja Abdullah, H. Adam, and A. R. H. Alhawari, "Compact narrowband bandpass filter using dual-mode octagonal meandered loop resonator for WiMAX application," *Progress In Electromagnetics Research B*, Vol. 16, 277–290, 2009.
6. Lin, T.-W., J.-T. Kuo, and S.-J. Chung, "Dual-mode ring resonator bandpass filter with asymmetric inductive coupling and its miniaturization," *IEEE Trans. on Microw. Theory and Tech.*, Vol. 60, No. 9, 2808–2814, 2012.
7. Zhang, S., L. Zhu, and R. Li, "Compact quadruplet bandpass filter based on alternative J/K inverters and $\lambda/4$ resonators," *IEEE Microw. and Wire. Comp. Lett.*, Vol. 22, No. 5, 224–226, 2012.
8. Zhang, S. and L. Zhu, "Synthesis method for even-order symmetrical chebyshev bandpass filters with alternative J/K inverters and $\lambda/4$ resonators," *IEEE Trans. on Microw. Theory and Tech.*, Vol. 61, No. 2, 808–816, 2013.
9. Lin, S.-C., "New microstrip cascaded-quadruplet bandpass filter based on connected couplings and short-ended parallel-coupled line," *IEEE Microw. and Wire. Comp. Lett.*, Vol. 24, No. 1, 2–4, 2014.
10. Feng, W. and W. Che, "Bandpass filter using open/shorted dual behaviour resonators," *Electronics Lett.*, Vol. 50, No. 8, 610–611, 2014.

11. Kumar, N. and Y. K. Singh, "Compact stub-loaded open-loop BPF with enhanced stopband by introducing extra transmission zeros," *Electronics Lett.*, Vol. 51, No. 2, 164–166, 2015.

12. Zong, B.-F., G.-M. Wang, J.-G. Liang, and C. Zhou, "Compact bandpass filter with two tunable transmission zeros using hybrid resonators," *IEEE Microw. and Wire. Comp. Lett.*, Vol. 25, No. 2, 88–90, 2015.

13. Park, J.-S., J.-S. Yun, and D. Ahn, "A design of the novel coupled-line bandpass filter using defected ground structure with wide stopband performance," *IEEE Trans. on Microw. Theory and Tech.*, Vol. 50, No. 9, 2037–2043, 2002.

14. Ma, K. and K. S. Yeo, "New ultra-wide stopband low-pass filter using transformed radial stubs," *IEEE Trans. on Microw. Theory and Tech.*, Vol. 59, No. 3, 604–611, 2011.

15. Ma, K., S. Mou, K. Wang, and K. S. Yeo, "Radial loaded transformed radial stub for LPF stopband extension," *Progress In Electromagnetics Research Letters*, Vol. 30, 125–132, 2012.

16. Singh, P. K., A. K. Tiwary, and N. Gupta, "Design and development of radial stub low-pass filter with improved characteristics," *10th Int. Conf. on Microw., Antenna, Propag. and Remote Sensing (ICMARS)*, 13–16, Jodhpur, India, 2014.

17. Tan, B. T., J. J. Yu, S. T. Chew, M.-S. Leong, and B.-L. Ooi, "A miniaturized dual-mode ring bandpass filter with a new perturbation," *IEEE Trans. on Microw. Theory and Tech.*, Vol. 53, No. 1, 343–348, 2005.

18. Mao, R.-J., X.-H. Tang, and F. Xiao, "Miniaturized dual-mode ring bandpass filters with patterned ground plane," *IEEE Trans. on Microw. Theory and Tech.*, Vol. 55, No. 7, 1539–1547, 2007.

19. Xu, J., Y.-X. Ji, W. Wu, and C. Miao, "Design of miniaturized microstrip LPF and wideband BPF with ultra-wide stopband," *IEEE Microw. and Wire. Comp. Lett.*, Vol. 23, No. 8, 397–399, 2013.

20. Fu, Z., K. M. Lum, and W. T. Koh, "Novel bow-tie bandpass filter design using multiple radial stubs," *PIERS Proceedings*, 1484–1487, Moscow, Russia, Aug. 19–23, 2012.

21. Xu, J., W. Wu, W. Kang, and C. Miao, "Compact UWB bandpass filter with a notched band using radial stub loaded resonator," *IEEE Microw. and Wire. Comp. Lett.*, Vol. 22, No. 7, 351–353, 2012.

22. Xu, J., "Compact quasi-elliptic response wideband bandpass filter with four transmission zeros," *IEEE Microw. and Wire. Comp. Lett.*, Vol. 25, No. 3, 169–171, 2015.

23. Ma, K., S. Mou, K. Wang, and K. S. Yeo, "Embedded transformed radial stub cell for BPF with spurious-free above ten octaves," *IEEE Trans. on Comp., Pack. and Manuf. Tech.*, Vol. 3, No. 9, 1597–1603, 2013.

24. Kwon, H., H. Lim, and B. Kang, "Design of 6–18 GHz wideband phase shifters using radial stubs," *IEEE Microw. and Wire. Comp. Lett.*, Vol. 17, No. 3, 205–207, 2007.

25. Goldfarb, M. E. and R. A. Pucel, "Modeling via hole grounds in microstrip," *IEEE Microw. Guided Wave Lett.*, Vol. 1, No. 6, 135–137, 1991.

26. Hong, J.-S. and M. J. Lancaster, *Microstrip Filters for RF/Microwave Applications*, Wiley, New York, USA, 2001.